

# A Fluorescent Dipyrinone Oxime for the Detection of Pesticides and Other Organophosphates

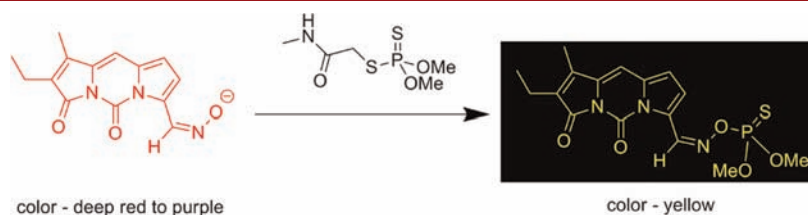
Ian Walton,<sup>†</sup> Marauo Davis,<sup>‡</sup> Lyndsay Munro,<sup>§</sup> Vincent J. Catalano,<sup>§</sup> Peter J. Cragg,<sup>||</sup> Michael T. Huggins,<sup>\*†</sup> and Karl J. Wallace<sup>\*†</sup>

Department of Chemistry, University of West Florida, 11000 University Parkway, Pensacola, Florida 32514, United States, Department of Chemistry and Biochemistry, University of Southern Mississippi, 118 College Drive, Hattiesburg, Mississippi 39406, United States, Department of Chemistry, University of Nevada, Reno, Reno, Nevada 89557, United States, and School of Pharmacy and Biomolecular Sciences, University of Brighton, Brighton BN2 4GJ, U.K.

mhuggins@uwf.edu; karl.wallace@usm.edu

Received March 28, 2012

## ABSTRACT



An *N,N*-carbonyl-bridged dipyrinone oxime has been synthesized and studied as a potential sensor for organophosphates. The molecular sensor underwent a drastic colorimetric response upon formation of the adduct. The pesticide dimethoate was found to produce the biggest spectral response, with a limit of detection equal to 4.0 ppm using UV–visible spectroscopy. Minimal fluorescence “turn on” via a PET mechanism was seen, and molecular modeling studies were used to explain the lower than expected PET response. The X-ray crystal structure of the fluorescent dipyrinone oxime was also obtained.

Organophosphorus compounds (OPs) are key components in agricultural pesticides and herbicides, which play vital roles in modern agriculture. However, the extensive overuse of these compounds has led to the poisoning of thousands of humans throughout the world. OPs, such as sarin and soman, have also been used as chemical-warfare agents. As a consequence, there is a need to develop

sensitive and selective receptors for the detection of said compounds.<sup>1–15</sup> The oxime functional group has been

<sup>†</sup> University of West Florida.

<sup>‡</sup> University of Southern Mississippi.

<sup>§</sup> University of Nevada, Reno.

<sup>||</sup> University of Brighton.

(1) Knapton, D.; Burnworth, M.; Rowan, S. J.; Weder, C. *Angew. Chem., Int. Ed.* **2006**, *45*, 5825–5829.

(2) Sun, J.; Guo, L.; Bao, Y.; Xie, J. *Biosens. Bioelectron.* **2011**, *28*, 152–157.

(3) Vandennebeele-Trambouze, O.; Mion, L.; Garrelly, L.; Commeyras, A. *6* 2001, 57–66.

(4) Viveros, L.; Paliwal, S.; McCraec, D.; Wildb, J.; Simonian, A. *Sens. Actuators B* **2006**, *115*, 150–157.

(5) Burnworth, M.; Rowan, S. J.; Weder, C. *Chem.—Eur. J.* **2007**, *13*, 7828–7836.

(6) Dale, T. J.; Rebek, J. J. *J. Am. Chem. Soc.* **2006**, *128*, 4500–4501.

(7) Dale, T. J.; Rebek, J. J. *Angew. Chem., Int. Ed.* **2009**, *42*, 7850–7852.

(8) Gotor, R.; Costero, A. M.; Gil, S.; Parra, M.; Martínez-Máñez, R.; Sancenón, F. *Chem.—Eur. J.* **2011**, *17*, 11994–11997.

(9) Liu, D.; Chen, W.; Wei, J.; Xuebing, Li, X.; Wang, Z.; Jiang, X. *Anal. Chem.* **2012**, *84*, 4185–4191.

(10) Paliwal, S.; Wales, M.; Goode, T.; Grimsley, J.; Wild, J.; Simonian, A. *Anal. Chim. Acta* **2007**, *596*, 9–15.

(11) Royo, S.; Martínez-Máñez, R.; Sancenón, F.; Costero, A. M.; Parra, M.; Gil, S. *Chem. Commun.* **2007**, 4839–4847.

(12) Candel, I.; Bernardos, A.; Climent, E.; Dolores Marcos, M. D.; Martínez-Máñez, R.; Sancenón, F.; Soto, J.; Costero, A.; Gilad, S.; Parraad, M. *Chem. Commun.* **2011**, *47*, 8313–8315.

(13) Guo, W.; Engelman, B. J.; Haywood, T. L.; Blok, N. B.; Beaudoin, D. S.; Obare, S. O. *Talanta* **2011**, *87*, 276–283.

(14) Obare, S. O.; De, C.; Guo, W.; Haywood, T. J.; Samuels, T. A.; Adams, C. P.; Masika, N. O.; Murray, D. H.; Anderson, G. A.; Campbell, K.; Fletcher, K. *Sensors* **2010**, *10*, 7018–7043.

(15) Royo, S.; Costero, A. M.; Parra, M.; Gil, S.; Martínez-Máñez, R.; Sancenón, F. *Chem.—Eur. J.* **2011**, *17*, 6931–6934.

integrated into the structure of pyridinium derived salts, which have been used in the treatment of OP poisoning.<sup>16</sup> Oxime antidotes bind to cholinesterase producing a reversible inhibition of acetylcholinesterase (AChE) and protects the enzyme against phosphorylation by OP compounds.<sup>17</sup>

Oxime containing moieties have been used by Anslyn<sup>18–20</sup> and others<sup>11</sup> as a means to detect OPs by incorporating oxime functional groups onto organic scaffolds that act as colorimetric, fluorescent, and chemiluminescent sensors. As part of our ongoing interests in the design and synthesis of novel fluorescent based sensors containing oxime functional groups, we have synthesized molecular targets **2** and **3**, based on a fluorescent *N,N*-carbonyl-bridged dipyrri- none (Figure 1).<sup>11,21–23</sup> The synthesis and a detailed conformational analysis study of compounds **1–3** have recently been reported.<sup>24</sup>

Solution studies on compound **2** found that the product exists as a mixture of *cis/trans* isomers in a 1:3 ratio, which is solvent independent, and the mechanism of *cis/trans* isomerism was also investigated.<sup>24</sup> Fortunately, X-ray

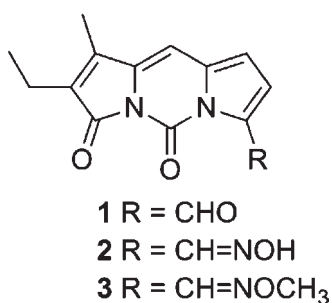


**Figure 1.** Fluorescent dipyrri- none target molecules.

quality crystals of the fluorescent dipyrri- none-derived oxime **2** in the *trans* form were obtained by heating a DMSO solution of **2** followed by standing for several days at room temperature. Interestingly, in the presence of a competitive hydrogen bonding solvent, such as DMSO, catemers (a linear hydrogen bonding motif) are formed by the weak C–H···O interactions between the C(10)–H on

(16) Shrot, S.; Markela, G.; Dushnitskya, T.; Krivovaya, A. *NeuroToxicology* **2009**, *30*, 167–173.

(17) Marrs, T.; Maynard, R.; Sidell, F. *Chemical Warfare Agents Toxicology and Treatment*; John Wiley & Sons: Chichester, 2007.

(18) Hewage, H. S.; Wallace, K. J.; Anslyn, E. V. *Chem. Commun.* **2007**, *38*, 3909–3911.

(19) Wallace, K. J.; Fagbemi, R. I.; Folmer-Andersen, F. J.; Morey, J.; Lynch, V. M.; Anslyn, E. V. *Chem. Commun.* **2006**, 3886–3–8888.

(20) Wallace, K. J.; Morey, J.; Lynch, V. M.; Anslyn, E. V. *New J. Chem.* **2005**, *29*, 1469–1474.

(21) Boiadjev, S. E.; Lightner, D. A. *J. Phys. Org. Chem.* **2004**, *17*, 675–679.

(22) Boiadjev, S. E.; Lightner, D. A. *Monatsh. Chem.* **2008**, *139*, 503–511.

(23) Brower, J. O.; Lightner, D. A. *J. Org. Chem.* **2002**, *67*, 2713–2716.

(24) Walton, I.; Davis, M.; Yang, L.; Zhang, Y.; Tillman, D.; Jarrett, W. L.; Huggins, M. T.; Wallace, K. J. *Magn. Reson. Chem.* **2011**, *49*, 205–212.

the central dipyrri- none ring and the oxygen atom of the oxime functional group (O(3)) of an adjacent molecule (Figure 2). The oxime OH and the C(9)–H on the pyrrole ring are hydrogen bonded to a single DMSO solvent molecule in the crystal. In addition, the crystal lattice displays a herringbone pattern with layers showing  $\pi$ – $\pi$  stacking between fluorescent dipyrri- none units with a separation of 3.353 Å, whereby the dipyrri- nones are rotated 180° such that the lactam and pyrimidone C=O moieties are located opposite each other (Supporting Information (SI), Figure S9).

The *N,N*-carbonyl bridged dipyrri- nones are typically bright yellow compounds with  $\lambda_{\text{max}}$  at ~400 nm and an  $\epsilon_{\text{max}}$  of ~20 000 L mol<sup>–1</sup> cm<sup>–1</sup> in CH<sub>3</sub>OH, DMSO, and CHCl<sub>3</sub> (SI, Table 1).<sup>23</sup> While the  $\lambda_{\text{max}}$  was only minimally impacted by changes in solvent polarity, the  $\epsilon_{\text{max}}$  was observed to be smaller in methanol in all cases. As previously observed, the substituents on the fluorescent dipyrri- none core can have a dramatic impact on the fluorescent quantum yields.<sup>21</sup> Compounds **1–3** fluoresced with varying quantum yields ( $\phi_{\text{F}}$ ) (SI Table 2). Although derivatives **2** and **3** had  $\lambda_{\text{em}}$  at ~500 nm with a  $\phi_{\text{F}}$  of ~0.3 in DMSO and CHCl<sub>3</sub>, quantum yields were approximately 50% lower in methanol. The aldehyde derivative, **1**, was essentially nonfluorescent;  $\phi_{\text{F}}$  was < 0.05 except in methanol. In order to understand its fluorescence in MeOH, electrospray mass spectroscopy (ESI-MS) experiments were conducted using methanol as the solvent. The experiments showed the formation of hemiacetal and acetal adducts at *m/z* = 262 and 276, respectively. Formation of such species provides a reasonable explanation for the increased fluorescence of **1** observed in methanol.

To determine whether the fluorescent dipyrri- none **2** acted as a colorimetric and/or fluorescence sensor for organophosphates, the oxime functional group had to be deprotonated to generate the oximate. The initial UV–vis solution of compound **2** (0.05 mol dm<sup>–3</sup>) in dry DMSO showed a  $\lambda_{\text{max}}$  at 420 nm. On addition of 20 equiv of

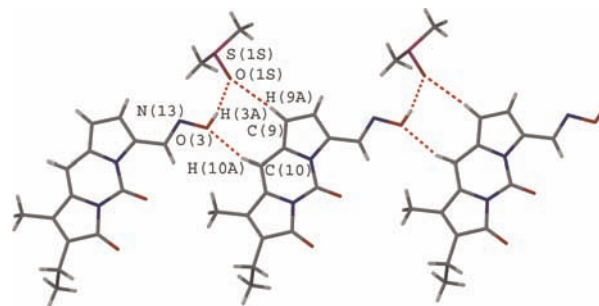


**Figure 2.** Crystal packing of compound **3**, illustrating the H-bonding catemer. The dashed lines are indicative of hydrogen bonding interactions. Donor–acceptor distances (Å): O(3)···O(1S) = 2.647; O(3)···C(10) = 3.178; and O(1S)···C(9) = 3.418.

Verkade’s base, a drastic color change was seen (*vide infra*). A broad band at  $\lambda_{\text{max}}$  at 573 nm was observed (Figure 3)

and assigned to the  $n\pi^*$  transition which is consistent with the formation of an anionic species.<sup>25</sup> Interestingly, the fluorescence spectra showed a slight blue shift in the emission band and only a marginal reduction in the fluorescence intensity (SI Figure S2B). Surprisingly, the fluorescence signal of **2** as the oximate ion with Verkade's base alone was still highly fluorescent.

In order to understand this phenomenon, the orbital energy level diagrams for compound **2**, as the oximate and the DFP-adduct, were investigated by density functional methods. The energy levels of the HOMO and LUMO in the ground state ( $\text{HOMO}_{(\text{gs})}$  and  $\text{LUMO}_{(\text{gs})}$ ) were calculated for each species by optimizing the ground state geometry to determine which orbitals participate in photoexcitation and photoluminescence ( $S_0 \leftarrow S_1$ ). The first excited states ( $\text{HOMO}_{(\text{ex})}$  and  $\text{LUMO}_{(\text{ex})}$ ) were computed using a time-dependent density functional model (Table 1).

The classical and generalized energy diagram for a PET sensing mechanism to occur has the HOMO of the donor group lying at a higher energy level of the  $\text{HOMO}_{(\text{gs})}$  of the fluorophore. This is certainly true in our system, whereby

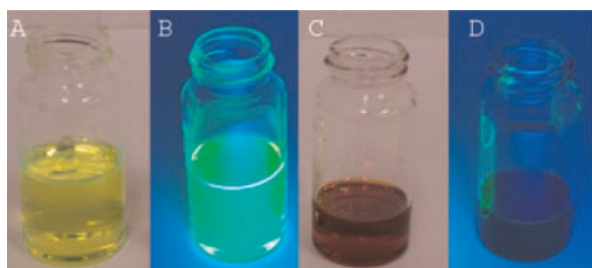


**Figure 3.** Photographs of oxime **2** (A and B) and **2**/oximate (C and D) in a  $\text{CH}_2\text{Cl}_2$  solution under incandescent and UV light, respectively.

**Table 1.** HOMO–LUMO Orbital Energies

compound	orbital energies (eV)			
	$\text{HOMO}_{(\text{gs})}$	$\text{LUMO}_{(\text{gs})}$	$\text{HOMO}_{(\text{ex})}$	$\text{LUMO}_{(\text{ex})}$
<b>2</b> –oxime	–5.572	–2.598	–3.793	–1.690
<b>2</b> –oximate	–0.993	0.885	–0.063	2.156
<b>2</b> –DFP adduct	–5.863	–2.801	–3.997	–1.886

the  $\text{HOMO}_{(\text{ex})}$  of **2**–oximate lies at 0.93 eV above the  $\text{HOMO}_{(\text{gs})}$  of the dipyrinone moiety. However, this energy difference does not efficiently quench the fluorescence via a PET mechanism as well as previously published fluorophores.<sup>26</sup>

On closer inspection of the orbital energy levels of compound **2** and the DFP adduct both the  $\text{HOMO}_{(\text{ex})}$

(25) Silverstein, R. M.; Webster, F. X. *Spectrometric Identification of Organic Compounds*, 6 ed.; John Wiley & Sons: Hoboken, NJ, 1997.

(26) Lakowicz, J. R. *Principles of Fluorescence Spectroscopy*, 3rd ed.; Springer: New York, 2006.

levels lie above the  $\text{HOMO}_{(\text{gs})}$  levels of their respective states. At first glance one would anticipate that the oxime and DFP adduct would both PET quench the fluorescence as their  $\text{HOMO}_{(\text{ex})}$  level is higher in energy than the  $\text{HOMO}_{(\text{gs})}$  level of their ground state, in contrast to other PET mechanisms where this level normally lies at a lower energy and thus the electron transfer process is unable to take place. Upon phosphorylation by DFP, the energies of these orbitals have shifted significantly ( $\Delta 1.86$  eV), reducing the PET quenching effect, but the fluorescence intensity remains unchanged. A similar energy difference between the  $\text{HOMO}_{(\text{gs})}$  and  $\text{HOMO}_{(\text{ex})}$  of compound **2** ( $\Delta 1.78$  eV) is observed. Clearly, the energy difference has increased which also prevented effective PET quenching. Information learned from the deprotonation studies was supported by molecular modeling calculations (SI, Figure S7).

UV–visible titration experiments using aliquots of organophosphates (diisopropylfluorophosphate (DFP), dimethoate, diisopropylchlorophosphate (DCP), and chlorfenvinphos, Figure 4), carbaryl (a commonly used insecticide), and two controls ((–)-nicotine and isodrine (a pesticide)) were conducted. The choice of base is important as strong and highly nucleophilic bases such as NaOH react with DFP to form the less toxic hydrolyzed product. Therefore, to avoid any competition between the bases and oximate **2** for DFP, a non-nucleophilic but strong base was required. A nitrogen–phosphorus superbases was used: Verkade's base (DMSO  $\text{p}K_{\text{BH}^+} = 33.6$ ). Consequently, the compounds were tested in a  $4.5 \times 10^{-4}$  mol  $\text{dm}^{-3}$  solution of **2**•Verkade's base in DMSO (Figure 4 and SI Figure S1). An excess of base (50-fold excess) is used in these experiments, as it is known that DFP is notoriously acidic, containing trace amounts of HF even when purchased fresh. It is also imperative that the solvents used for the titrations are dry; otherwise hydrolysis of the oxime can occur. Based on NMR observations, wet solvents (DMSO,  $\text{CDCl}_3$ , etc.) lead to slow hydrolysis resulting in a mixture of **1** and **2** being present over the course of a 2–3 h time period.

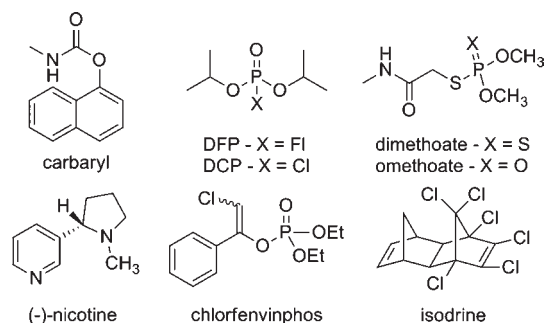


**Figure 4.** Organophosphates and other reactive compounds.

Upon the gradual addition of aliquots of a reactive titrant to the solution of **2** with Verkade's base, the 420 nm absorption band was hypsochromically shifted to  $\lambda_{\text{max}} \sim 405$  nm while growing in intensity and the 561 nm band disappeared. A representative titration of dimethoate into

a solution of the oximate of **2** is shown in Figure 5A. The lack of a true isosbestic point at  $\sim 460$  nm can be explained by the reactive nature of the oximate/dimethoate adduct which decomposed to form additional products. The changes occurring in these two absorption bands can be used as a signature for sensing the presence of other reactive species. A plot of the ratio intensity at 405 nm/561 nm (Figure 5B) shows that the controls, isodrine and (–)-nicotine, had a response ratio of less than  $\sim 2$  at 4 equiv of titrant while omethoate and dimethoate showed the greatest response with ratios of 26.7 and 36.2, respectively. Dimethoate had a response ratio 30 times that of (–)-nicotine and 17 times that of isodrine to the oximate of **2**. These results indicate selectivity of the system for the more reactive organophosphates and carbamate derivatives compared to the controls.

The same titration studies were conducted and analyzed by changes in fluorescence intensity. The results show the greatest change in fluorescent intensity for carbaryl (SI, Figure S6) as a consequence of the anionic naphthonal ( $C_{10}H_7O^-$ ) species being formed. The naphtholate ion had a very strong, broad emission band at 495 nm in agreement with other literature work<sup>27</sup> and is formed by nucleophilic attack on the probe (**2**) and carbaryl (Figure 4). As expected, based on the previous discussion, the fluorescent response for the other reactive species was uninteresting.

To determine the limit of detection (LoD) a least-squares regression of  $y$  (absorbance units) on  $x$  (concentration) was calculated, taking into account the statistic ( $S_{y/x}$ ). This value was then used to calculate the standard deviation for the slope and the intercept. The confidence limit of the slope is defined as  $b \pm t_{s_b}$ , where  $t$  is the  $t$ -value taken from the desired confidence level and  $n - 2$  degrees of freedom. In our experiment we chose the 95% confidence level ( $t$ -value = 2.57,  $(n - 2) = 5$ ). Therefore the LoD is calculated from  $y = y_B + 3S_B$  (SI, Figure S8). The LoD for dimethoate was found to be  $4.0 \times 10^{-6}$  M or 4.0 ppm.

A control experiment was carried out with methyloxime **3**. No change in color or fluorescence was observed upon the addition of DFP, confirming the need of the oximate to undergo the phosphorylation reaction (SI Figure S3B).

In summary, fluorescent dipyrinone **2** instantaneously produced a distinct crimson red color (561 nm) upon deprotonation with a strong base, which disappeared on the addition of organophosphates or pesticide. Even though the fluorescence “turn off” was not shown to be as significant as that for other fluorophores, a modest fluorescent “turn on” was observed upon phosphorylation of DFP.

(27) Kumar, A. C.; Mishra, A. K. *Talanta* **2007**, *71*, 2003–2006.

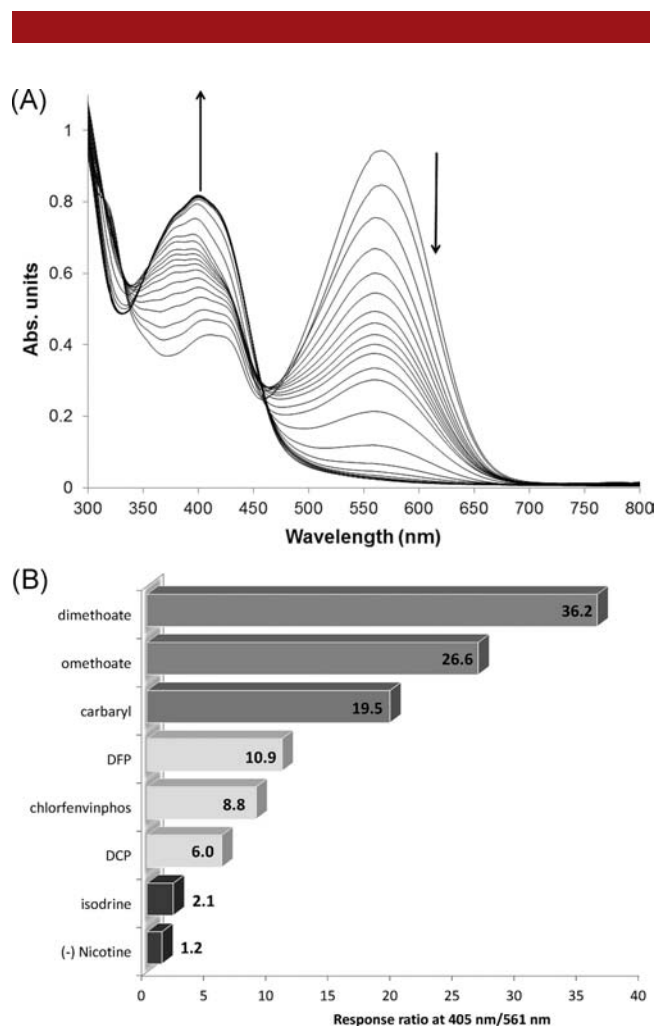


**Figure 5.** (A) UV–visible titration of oximate of **2** with dimethoate. (B) Graph of response ratio for absorption peaks at 405 and 561 nm and 4 equiv of the reactive species.

**Acknowledgment.** The K.J.W. research laboratory is grateful for financial support from NSF Grant Nos. OCE-0963064 and CHE-084039, SERRI (southeast region research initiative) 63892, and the McNair Scholarship at Southern Miss for the support of the undergraduate student Marauo Davis.

**Supporting Information Available.** Binding analysis (UV–vis and fluorescence), molecular modeling calculations, and X-ray data. This material is available free of charge via the Internet at <http://pubs.acs.org>.

The authors declare no competing financial interest.